Turning Wine (Waste) into Water: Toward Technological Advances in the Use of Constructed Wetlands for Winery Effluent Treatment

Craig Sheridan, Diane Hildebrand, and David Glasser
School of Chemical and Metallurgical Engineering, University of the Witwatersrand, Johannesburg, South Africa

DOI 10.1002/aic.14297
Published online December 4, 2013 in Wiley Online Library (wileyonlinelibrary.com)

The research presented in this article describes an investigation into the use of vegetated submerged reedbeds (VSR) as a practicable alternative for effluent treatment for small-scale wine producers. In this study, we found that the hydraulic processes occurring within the VSR display significantly nonideal behavior. If the feed to the VSR was located on the surface the dead volume accounted for approximately 25% of the nonideal behavior of the system and bypass accounted for a further 6%. A preferential flow pattern was found within the VSR with the greatest flow occurring closest the surface and in the center, and the least at the sidewalls. We propose that the flow profile can be conceptualized as being hull shaped and found that this profile was the same for irregularly shaped gravel and for spherically shaped gelatinous beads. We, therefore, hypothesize that it is not dependent on the geometry of the VSR or the packing medium. © 2013 American Institute of Chemical Engineers *AIChE J*, 60: 420–431, 2014
Keywords: constructed wetlands, hydraulic processes, reactor model, winery waste treatment

Introduction

Winemaking in South Africa is primarily restricted to the winter rainfall and semiarid areas of the Western and Northern Cape provinces. Geographically, these areas are characterized by low population densities (excepting the metropolitan area of Cape Town) and limited water resources. Farms often rely on farm-dam or spring water, the supply of which is highly variable. Those farms located near the Cape Town metropole can access municipal water from the Theewaterskloof Dam, which is situated within 100 km of Cape Town, but this water is expensive, and farmers are competing with human and industrial consumption needs.

Winemaking is very similar to conventional chemical engineering. The process begins with a raw material (in this instance grapes). Some kind of beneficiation or size reduction process is conducted to speed up the rates of chemical reaction, which in winemaking is the conversion of glucose and fructose to ethanol. This yields a product—wine. As with all other industries, winemaking creates waste streams and as with all other chemical industries, these must be disposed of. Solid waste (such as stems, pips, grape skins, etc.) can be sustainably converted into soil amendments (such as composts) and the waste water must be treated as it is very concentrated in organic matter. For sustainable winemaking, the process needs to be assessed holistically. Decisions must consider the impact on the quality of the product as well as the environment. A more complete discussion on sustainable winemaking is given by Sheridan.[1]

The water that enters the process that converts grapes into wine will leave as wastewater (since in South Africa it is illegal to add water to wine). The wastewater contains spillages from processing and handling, the residues of washing the tanks, intentionally drained wet waste products such as lees, and potentially other contaminants, such as agricultural manure. All wineries are expected to conform with legislation relating to the treatment or disposal of waste streams.[2–5] Thus, if a winery discharges effluent into a sewer, it must ensure that it is under the maximum allowable limit on the chemical oxygen demand (COD) and the quantity of sodium it contains, as these are the criteria most relevant to winery effluent.[6] The specific parameters applied will depend on the requirements of the municipality that manages the sewer. Conversely, if the wastewater is to be released to the environment, the permissible strength of the chemicals in the waste will be governed by national rather than local legislation, although it will also depend on whether the environment in question is pristine or not.

Many wineries (46%) are small, and press less than 100 tons of grapes per annum.[7] Thus, using the method developed by Sheridan[1] we can assume that just under half of all wineries in South Africa consume fewer than 1000 L of water per day and produce a corresponding quantity of effluent. These small wineries can be licensed to irrigate their wastewater to a pasture, provided both that the COD does not exceed 5000 mg/L and that they irrigate less than 50 m^3 per day.[3] The Department of Water Affairs (DWA) discourages this practice, even by those who comply with the limit, because it is considered wasteful of water. The DWA would

Correspondence concerning this article should be addressed to C. Sheridan at craig.sheridan@wits.ac.za

prefer to see water treated and reused or returned to a water resource than irrigated where it is irrevocably lost from the catchment.

Because many wineries exceed the limits described above in terms of COD,[1] they are required to treat their wastewater by some form of processing before releasing it. Winery wastewater treatment techniques are diverse, but all have the same goal, which is to reduce the COD. Treatment technologies include using sequencing batch reactors, aerobic digestion, anaerobic digestion, rotating biological contactors, settling ponds, and constructed wetlands (CWs).[1,8] With the exception of the last, all these systems are capable of almost full effluent treatment. However, the technologies are costly, and require staff trained to operate and control them. The smaller wineries in particular cannot afford to use such specialized kinds of personnel, and therefore, cannot use these sophisticated systems reliably.

This is the reason why, in the research described here, we chose to investigate the last and most under researched of the waste treatment options described above, in this case, the use of vegetated submerged reedbed (VSR) type CWs. There are a number of reasons, apart from cost saving and the relative simplicity of the technology involved, for believing that a CW offers the best option for small-scale wineries. Some of these are technical, for example:

- it is a low-maintenance treatment system;
- the treated water can be reused; and
- preliminary tests indicate that CW plants can thrive in the effluent created by wineries.

However, a living treatment system is not only effective but offers a number of benefits in a wider, environmental and social context, which include but are not restricted to:

- the aesthetic qualities of a CW;
- its production of biomass-like cut flowers and thatching materials;
- the potential use of this biomass to provide a means of livelihood to low-income farming communities (a significant factor in a developing country); and
- the creation of a space whereby a treatment system becomes a habitat for wetland fauna and flora and the generation of some biodiversity.

In South Africa, the use of CWs for winery effluent treatment is a very recent development. At present, there are only a few such systems in existence. The design briefs for these systems are mostly heuristic, that is, they remain at the mathematical rules-of-thumb stage. We conducted our research on the basis of just such a CW, which had been constructed by the agricultural research council (ARC) at their Nietvoorbij Campus in Stellenbosch. Our aim was to conduct experiments to determine the properties of treatment process (listed below), and to use these to establish more rigorous design principles. The initial research investigated the aspects of winery effluent treatment we considered most significant.

1. The composition of winery effluent and its temporal variations: what does it consist of, how does it change over the duration of a harvest period, and how does it change over the course of the year? Answering these questions required analysis of the effluent over a full year.
2. The behavior of effluent flowing through the CW: is there any bypass of flow or "dead" volume within the CW that makes it less efficient? These data were obtained by running a tracer impulse-response experiment, by means of which we measured the mean residence time and the dispersion within the system. This method was also used to identify whether the CW behaved like a plug flow, stirred tank reactor or series of stirred tank reactors, or any combination thereof.
3. The rates at which the components of winery effluent are degraded. Answering this question required the use of the data obtained from both one and two above.

If we could answer points one to three, we hoped to be able to develop a model that would predict the behavior of the system accurately. This could then be used to design new VSRs that treat winery effluent more efficiently than the existing models. Conversely, we recognized the possibility that the experimental results might indicate that the treatment process is too complex to make prediction feasible. Even if the latter proved to be the case, we reasoned that our findings would yield data that had not been considered before, such as the rates of decomposition of the winery effluent components. Both would be useful to designers of VSRs.

As indicated above, the research was broken into three segments. The first portion was an analysis of winery effluent. A report on this article has already been published,[9] but to sum up our most significant results, we found that in the winery effluent tested, ethanol comprised approximately 90% of the COD, and that ethanoic acid constituted most of the rest. (Other minor organic components of the effluent included propanol, propionic acid, and butanoic acid. The principal inorganic constituents of the effluent were sodium and potassium. Nitrate and phosphate were present, but in insignificant amounts.) The COD was variable, and could be directly related to the number of tons of grapes harvested. However, we seldom encountered COD concentrations higher than 7000 mg/L during our investigation.

The second portion of the research involved an investigation into the hydraulic behavior of the VSR, which forms the subject of this article. To our knowledge, this is the first study of this kind on a CW system being used to treat winery effluent. The findings were of interest because they showed that the flow profile had a distinctive shape that suggested the presence of "dead areas" in the movement of effluent through the VSR. We, therefore, devised methods by means of which the flow rate (and with it the overall treatment capacity of the VSR) could be raised to optimal efficiency. In the third section, we measured and interpreted the rate constants of the processes of degradation. This topic too will be presented in a separate article.

Modeling constructed wetland systems

For approximately a century, CWs have been used to provide biological treatment for wastewaters and effluents.[10] These constructions are typically packed with gravel, custom packing materials such as high-surface area media, or packing plates.[11] Vegetated trickle bed filters (also referred to as vegetated submerged reedbeds—VSR, or horizontal subsurface flow CWs) are a type of trickle bed filter, which is colonized by macrophytes on the surface. VSRs can be successfully modeled using fundamental chemical engineering theory.[6,12–20] If the flow is assumed to be ideally mixed, the system can be modeled on that of a continuous stirred tank reactor (CSTR). If the flow is assumed to behave like an ideal plug, the system would follow the model of an ideal plug flow reactor (PFR). Other types of reactor model are

Table 1. Regression Equations for the Removal of COD or BOD in CWs (Adapted from Ref. 28)

Number	Equation	r^2
1	$C_{Out}=(0.11\,C_{In})+1.87$	0.74
2	$C_{Out}=(0.33\,C_{In})+1.4$	0.48
3	$C_{Out}=502.2\,e^{-0.111T}$	0.69
4	$C_{Out}=(0.099\,C_{In})+3.24$	0.33
5	$L_{Removed}=(0.653\,L_{In})+0.292$	0.97
6	$L_{Out}=(0.145\,L_{In})-0.06$	0.85
7	$L_{Out}=(0.13\,L_{In})+0.27$	0.57
8	$L_{Out}=(0.17\,L_{In})+5.78$	0.73

described in the literature.[21] In practice, few reactors are ideal, and phenomena such as dispersion, diffusion, dead zones, and short circuiting of the fluid are relatively commonplace.[22] In VSRs, the flow regime may be typical of neither a PFR nor CSTR, but display characteristics of both. This implies that the time that the reactants remain inside the reactor may be significantly different from that envisaged in the design criterion. Therefore, measuring the residence time distribution (RTD) of the reactor and determining the mean residence time are necessary for accurate model description.

Kinetic vs. Hydraulic Formulae as Reactor Models. The literature on the subject describes different types of mathematical formulae for CWs, but these can be broadly broken into four types: empirical, kinetic, hydraulic, or a combination of kinetic and hydraulic.

Regression analysis has been used to model CWs at least since the early 1990s.[23–27] Some of these correlations are given in Table 1. These relationships relate to either the load of the effluent applied to the CW or to the concentration of the effluent.

As a thought experiment we have used these equations to calculate the outlet COD from a CW treating an influent of 100 mg/L of COD. We present the outlet COD for this hypothetical CW in Figure 1. It is clear from this plot that substantially different effluent degradation is predicted (±300%) by using the different regression correlations. For design purposes, the choice of equation would be something of a lottery and the chances of the resulting CW working would, therefore, also be unknown.

Kinetic equations are used to describe the outlet concentration, usually as a function of the inlet concentration and the rate constant, k, which is sometimes expressed in different ways, for example, the time-dependent retardation model.[29] Hydraulic equations are normally derived from investigation of the way in which the wastewater flows through the CW. Applying such a mathematical formula yields information on the mean residence time and the degree of dispersion, which can then be used to arrive at a conceptual reactor that determines the outlet concentration. This is a function of many variables such as inlet concentration, the length of the CW, the velocity of the rate at which the fluid passes through it, the rate constant, and the degree of dispersion, D or the Peclet Number, Pe. The Peclet number is essentially a ratio of advective to diffusive transport and is, therefore, the ratio of a characteristic length multiplied by velocity which is divided by the diffusivity. Depending on the type of reactor described (a plug flow or tanks-in-series), the dispersion number can also be used to calculate the number of tanks, N. Finally, there are some reactors that require a component of kinetic and hydraulic modeling. An example of such a reactor is presented in this article, as indicated by the partial tanks in series (PTIS) model shown in Table 2.

A summary of a number of these models is presented in Table 2, which is adapted from that drawn up by Villaseñor et al.[13] where

$$q=\sqrt{1+\frac{4\cdot Da}{Pe}} \tag{1}$$

$$\text{and the Damkohler Number } Da=\frac{l\cdot k}{u} \tag{2}$$

The kinetic formulae shown here which assume that the flow regime is ideal, introduce an error that may be significant under certain conditions. In addition, researchers using the retardation model, for example, seek to explain a change in the rate constant in terms of actual time spent in the reactor. (This should be distinguished from the mean residence time, which is the calculated average of the distribution of times for the entire contents of the effluent stream to pass through the reactor.) We consider this approach misplaced because lumped parameters (such as COD) will always display this type of behavior. The change in rate of reaction is easily explained by observing that the more readily biodegradable substances in the COD (such as glucose) react quickly in comparison with the more recalcitrant substances it contains, like ligno-cellulosic materials. Believing that a more fruitful approach is to explain the effluent stream fully by characterizing the components of lumped parameters, and to determine the different rate constants of the individual constituents, we have carried out the research and published our findings on the constituents of the effluent.[9]

A kinetic or hydraulic model of a reactor can be used for describing the processes that occur in a CW. As noted, we have chosen the latter.

Finding the internal age distribution and calculating some hydraulic parameters

For a more detailed description of the methodology of conducting impulse-response tracer studies and the mathematical processing of the resulting data, the reader should refer to either Fogler[22] or Levenspiel[21]. A tracer study needs to be done to determine the hydraulic parameters of any reacting system. Although this is normally conducted as an impulse-response tracer experiment, it can also be carried out as a step-change experiment. Both can be interpreted to

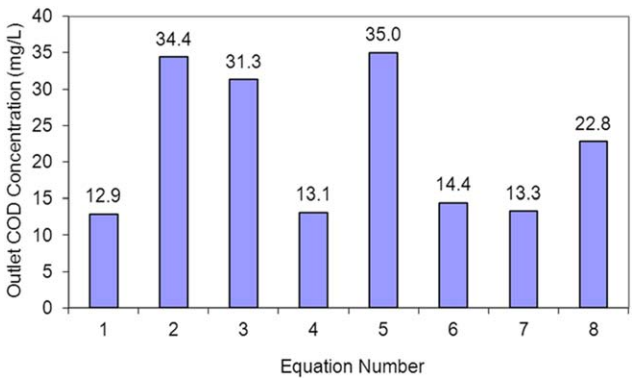

Figure 1. Variation of the outlet concentration for a given inlet concentration of 100 mg/L COD for the correlations presented in Table 1.

[Color figure can be viewed in the online issue, which is available at wileyonlinelibrary.com.]

Table 2. Different CW Models Presented as Either Being Kinetic or Hydraulic in Method

Hydraulic Model→ Kinetic Model ↓	Ideal Plug Flow	Plug Flow with Dispersion	Tanks-in-Series
k-C	$\frac{C_{Out}}{C_{In}}=e^{-kt}$	$\frac{C_{Out}}{C_{In}}=\frac{4\cdot q\cdot e^{\left(\frac{Pe}{2}\right)}}{(1+q)^2\cdot e^{\left(\frac{Pe\cdot q}{2}\right)}-(1-q)^2\cdot e^{\left(\frac{Peq}{2}\right)}}$	$\frac{C_{Out}}{C_{In}}=\frac{1}{(1+k\tau)^N}$
k-C*	$\frac{C_{Out}-C^*}{C_{In}-C^*}=e^{-kt}$	$\frac{C_{Out}-C^*}{C_{In}-C^*}=\frac{4\cdot q\cdot e^{\left(\frac{Pe}{2}\right)}}{(1+q)^2\cdot e^{\left(\frac{Pe\cdot q}{2}\right)}-(1-q)^2\cdot e^{\left(\frac{Pe\cdot q}{2}\right)}}$	$\frac{C_{Out}-C^*}{C_{In}-C^*}=\frac{1}{(1+k\tau)^N}$
Retardation[29]	$\frac{C_{Out}}{C_{In}}=\frac{1}{(1+bt)^{Ke/b}}$	N/A	N/A
Partial tanks in series[19]	$\frac{C_{Out}}{C_{In}}=\frac{1}{\left(1+k_{app}\frac{\bar{t}}{P}\right)^P}$		
Spatial tanks in series[16]	$\frac{C_{Out}}{C_{In}}=\frac{1}{\left(1+k_i\cdot\frac{2}{3}\cdot\frac{l\cdot d\cdot w}{F\cdot N}\right)^N}$		
ZDM[12]	Zones of diminished mixing		
OTIS[30]	One-dimensional transport with Inflow and Storage		

provide mean residence times, degree of dispersion, and so forth. The internal age or RTDs indicate the length of time that each molecule spends in the reactor. Some molecules will follow a short circuit from the feed to the outlet, whereas others will get caught up in dead volumes (i.e., those parts of the VSR with zero flow). Both of these are discrepant from those that travel exactly as specified in the design brief. Because these particles take different paths, they spend varying amounts of time in the reactor. The distribution of these times can be plotted upon a graph (see Fig. 4).

The shapes of the distribution presented in Figure 4 have significant statistical properties. The first moment of the age distribution is by definition the mean residence time, $\bar{t}_m$ (see Eq. 3), and the second moment is notated as σ^2, which is calculated according to Eq. 5. If the second moment is normalized, σ_θ^2 (Eq. 5), it can be used to calculate the Peclet number (Pe), $1/Pe$, which is the dispersion number (D) or the number of tanks, N, for a CSTR in series model.

$$\bar{t}_m=\sum_{i=1}^{n} t_i\cdot(t_i-t_{i-1}) \tag{3}$$

$$\sigma^2=\left[\sum_{i=1}^{n} t_i^2\cdot E_i\cdot(t_i-t_{i-1})\right]-\bar{t}_m \tag{4}$$

$$\sigma_\theta^2=\frac{\sigma^2}{\bar{t}_m}^2 \tag{5}$$

$$\sigma_\theta^2=2\cdot D-2\cdot D^2\cdot\left(1-e^{-1/D}\right) \tag{6}$$

$$N=1/\sigma_\theta^2 \tag{7}$$

For packed-bed reactors (essentially plug flow with dispersion), the Peclet equation has been solved for first-order reactions.[21] In terms of conversion X, the rate constant is k; the Peclet number, Pe; the length of the system, l; and the velocity of the impulse, u, the Peclet equation is expressed as

$$X=1-\frac{4\cdot q\cdot e^{\left(\frac{Pe}{2}\right)}}{(1+q)^2\cdot e^{\left(\frac{Pe\cdot q}{2}\right)}-(1-q)^2\cdot e^{\left(\frac{Pe\cdot q}{2}\right)}} \tag{8}$$

This equation has been used successfully by others[12,18,30] to describe VSRs (as they are normally packed beds), and is shown in Table 2. VSRs are typified by a single-mode RTD with a characteristic long tail. The greater the value of D, the more nonideal the flow within the system is.

Other methods for describing nonideal flow have been reported in the relevant literature.[31] Perrson et al. in particular discusses the ratio of the measured residence time to the ideal residence time and define an effective volume ratio as a function of the length to width ratio. This is given as

$$V_{\text{eff}}=\frac{\bar{t}_m}{V/_F} \tag{9}$$

This is a ratio of the residence times and not the volumes, because the authors felt that it was impossible to measure the dead volume directly. They also defined a hydraulic efficiency factor, λ, by means of which it is possible to compare different designs of reacting VSRs. This hydraulic efficiency factor is given by Eq. 10, where N is the number of tanks in the TIS model.

$$\lambda=V_{\text{eff}}\,(1-1/N) \tag{10}$$

These parameters are used for comparison in this article, to match against those used for our assessment of nonideal behavior.

The focus of the research experiment described in this article is threefold: to report on the data we measured; to develop a hypothesis from the data obtained; and to test it. There are four components to the hypothesis.

- There is a preferential flow pattern within a VSR, with the greatest flow occurring closest the surface and in the center, and the least at the sidewalls, if the flow is applied to the surface of the VSR at the feed position. This is conceptualized as a hull-shaped velocity profile.
- The hull-shaped profile is formed irrespective of the shape of the packing medium.
- We can reproduce this hull-shaped profile in a laboratory-scale experiment using spherically shaped packing.
- The profile can be changed by altering the location of the feed, and the dead volume can be significantly reduced by introducing a fully distributed feed and outlet system.

Table 3. Engineering Design Specifications of the VSR

Design Specification	Value
Length	40 m
Depth	1 m
Width	4 m
Lining	Plastic pond liner
Hydraulic gradient	Approximately 2%
Soil matrix	Dolomitic gravel
Average matrix particle size	Approximately 20 mm
Matrix void fraction	40%

If our hypothesis is correct, the design of a CW could potentially be optimized by ensuring that the flow is properly distributed. This has the potential to result in smaller CWs with concomitant cost reductions and reduced land requirements.

Experimental programme

In this study, we conducted experiments in two stages. In the first, we investigated the existing VSR at the ARC Nietvoorbij in Stellenbosch, South Africa. We performed an impulse-response tracer experiment, analyzed the moments of the resulting distributions, and used these data to develop a hypothesis on the flow characteristics of the system. We then tested our hypothesis by carrying out another impulse-response tracer experiment on a transparent laboratory-scale packed-bed reactor, and analyzing the moments of the resulting distribution. For testing our hypothesis, we built a glass reactor and filled it with florists' polymer-based gelatinous balls that are roughly spherical in shape, approximately 10–15 mm in diameter, and transparent. The rectangular glass reactor had nine dispersed inlet and outlet positions, and the inlet and outlet flows could be varied between using any one port and all ports simultaneously. We controlled the flow into the reactor and formed the impulse by an injection of tracer into the feed line. The reactor setup allowed us to observe where the tracer was going, and to identify where the bypass and dead zones could be found. In both experiments, flow was observed to be laminar.

Materials and Methods

Description of the experimental rigs/apparatus

Description of the Physical Properties of the VSR at the ARC, Stellenbosch. This VSR, which was built in about 2001, is a subsurface flow CW 40-m long, 4-m wide, and 1-m deep. It was built on a slope with a gradient of approximately 2%, was lined with black polyethylene pond-lining film, and filled with dolomite gravel ($CaMg(CO_3)_2$) with a mean particle diameter of 0.02 m and a void fraction of approximately 40%.

The design specifications for the VSR are presented in Table 3.

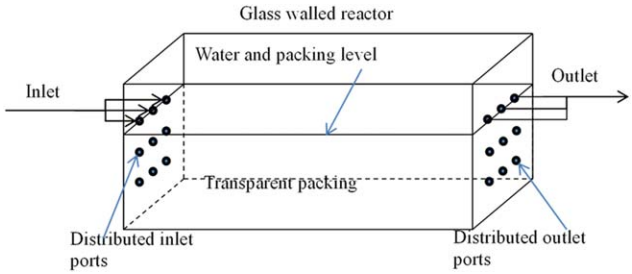

Figure 3. Laboratory apparatus used to test bed efficiency.

[Color figure can be viewed in the online issue, which is available at wileyonlinelibrary.com.]

Fourteen sample ports constructed from a flexible polyvinyl chloride (PVC) mesh were installed in the VSR for the purposes of this study. These flexible mesh strips were wrapped around a 100 mm PVC pipe, joined and submerged vertically to a depth of 1 m. The PVC pipes were then removed, leaving the mesh in place. Because it is inherently stable, the gravel did not collapse or force the closure of any sample ports at any time during the investigation. This feature of the design ensured that the sample ports did not impede the flow through the VSR. The grid of sampling ports was designed according to the published methodology given by Popek.[32] A schematic diagram showing the side and top views of the VSR is given in Figure 2. All the tailings were fed through sample port 5 into an open collection pond. Two meters were installed, a rain gauge and a water meter to measure the feed flow rate.

The VSR was originally planted sparsely with *Phragmites australis*, which partially colonized the surface as it grew. This planting also included a small number of ornamental plants, such as *Zantedeschia aethiopica*, *Chondropetalum tectorum,* and *Cyperus papyrus*, on a trial basis. We renovated the feed line to ensure the flow would be distributed as evenly as possible onto the surface at the entry-point end of the VSR.

Description of the Laboratory-Scale Packed-Bed Reactor. For this experiment, we constructed a transparent glass reactor, 250-mm high, by 250-mm wide by 500-mm long. The tank had nine inlet and nine outlet ports drilled into the sidewalls at the height to which the packing would fill the reactor. This would allow us to simulate any choice of flow pattern including flow along the top of the bed. We used transparent polymer gel beads as the packing material. A sufficient number of the beads were placed in the tank to reach the height of the inlet ports—150 mm, and these were hydrated in water. The tank had a total volume of 18.8 L and the polymer beads had a measured void fraction of approximately 0.48. Thus, the liquid volume was approximately 8.1 L. A schematic of the apparatus is shown in Figure 3.

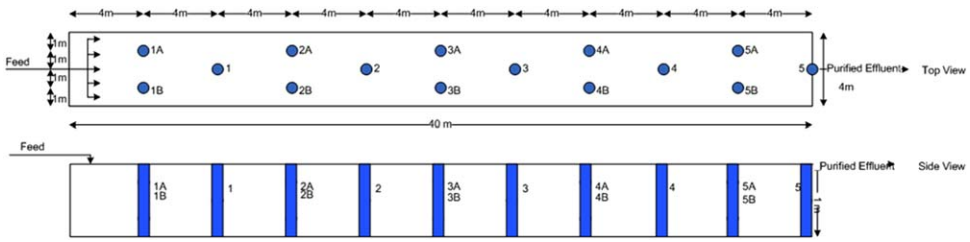

Figure 2. Schematic diagram of the VSR showing a side and a top view.

[Color figure can be viewed in the online issue, which is available at wileyonlinelibrary.com.]

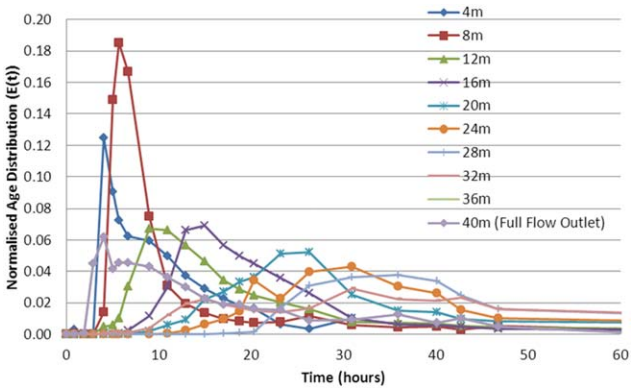

Figure 4. Normalized age distributions showing the progression and dispersion of the pulse as it moves through the VSR (with lateral variation averaged).

[Color figure can be viewed in the online issue, which is available at wileyonlinelibrary.com.]

Conducting the impulse-response experiments

Tracer Experiments at the ARC VSR. We selected a dose of potassium bromide as the tracer to be pulsed through the VSR for the impulse-response experiment. The reasons for this choice were that bromide is highly soluble, is not adsorbed to or absorbed by the dolomitic matrix of the filter, is generally nonreactive, can be readily analyzed and was an alien anion in the system we were studying. Before we injected the pulse, we took a reference sample at each port to record the environmental baseline. 5 kg of the tracer was mixed with 20 L of water and injected as an impulse into the feed line. During the experiment, water from a farm irrigation point was fed into the system to ensure the influent was as constant as possible. It is a recognized limitation of this experiment that the flow varied to some degree, because the water pressure was provided by a farm pump which had to meet competing demands. The data we obtained were used to find the RTD, which in turn made it possible for us to calculate the RTD, an age distribution ($E(t)$), for each of the sample ports.

Tracer Experiments on the Lab-Scale Rig. For this laboratory experiment, we chose FWT Red (Bright Dyes) as the tracer, as we were seeking to observe the flow patterns. We prepared a solution of 1000 mg/L of the dye and injected an impulse of 20 mL of this solution into the reactor. The flow was held constant at 7.3 L/h throughout this experiment.

Sampling protocol

Sampling Regime at the ARC. The VSR was divided into a number of sample wells, as depicted in Figure 2. Sample aliquots of 500 mL were taken from each sample point at intervals of approximately 1 h for the first 6 h; every 2 h for the next 18 h; and every 4 h for the following 24 h. A penultimate sample was taken at 64 h, and a final sample at 200 h.

Sampling Regime on the Lab-Scale Reactor. We took the samples for this experiment at the point where the three outlet lines had converged, to smooth any lateral variation. The samples of 20 mL aliquots were taken at irregular intervals, but were timed to ensure we obtained the most valuable data. In other words, we took many more samples when significant change was most likely to occur. The final sample was obtained at 180 min.

Analytical methods

Analysis of KBR Samples Taken from the VSR. The sample aliquots were analyzed within 48 h of being taken. We analyzed the samples for bromide (Br^-) using high performance liquid chromatography (HPLC) with a Waters IC-Pak (HR 4.6 $\times$ 75 mm) anion column. The HPLC was fitted with a conductivity detector. During analysis, we kept the column at ambient temperature and used 1.5 mL per min of mobile phase containing 3.6 mM of sodium carbonate. The resultant data were calibrated by applying preprepared standards.

Analysis of FWT Red Samples Taken from the Lab-Scale Reactor. The samples taken from the lab-scale reactor were not pretreated in any way. They were transferred into plastic cuvettes, and analyzed using a Merck Spectroquant at a wavelength of 550 nm (according to the dye manufacturer's specification). The resultant data were calibrated according to preprepared standards.

Results

The calculation of hydraulic properties of the VSR

The Calculation of the Internal Age Distributions [E(t)] for the VSR at Each Sample Port. An initial inspection of the breakthrough curves indicated that there was little difference between the left- and right-hand side (A and B) sample ports, which implies that there is little lateral variation of the flow across the width of the VSR. Therefore, the data for these locations (A and B ports) were averaged. The resultant data, shown in Figure 4, are a series of distributions. These illustrate the processes of dispersion (the long tail of the distribution) and short circuiting (multimodal distributions) of the effluent through the VSR. The mass-balance recovery of tracer ranged between 11 and 24% at differing locations across the system. The presence of multimodal distributions indicates that some short circuiting or bypass is occurring within the VSR. This data agree with experiments conducted on trickle flow in packed columns[33] and confirm that VSRs are similar to flooded trickle flow reactors displaying dead volumes and bypass.

Calculation of Hydraulic Properties from the Age Distribution. The first moment of the normalized age distribution was used to calculate $\bar{t}_m$ and V_{eff} and the second moment to calculate the Peclet Number (Pe). The results of these calculations are presented in Table 4, as are the modes (the location of the peaks) of the distributions.

These data indicate that the pulse dispersed with increasing length, and that some degree of bypass occurred. The bypass (or short circuiting) is indicated by multimodal distributions, and this is most clearly evident in sample port 5 (at 40 m), through which the entire flow passed. The distributions of sample ports 4 and 5 (showing the greatest degree of bypass) are shown in Figure 5. The time for the pulse to pass, and concentration are represented by the peaks in this chart.

The short circuiting observed, particularly toward the end of the VSR, could be attributed to inadequate baffling at the sidewalls and bottom during construction, which would allow flow channels to be created. The effluent would use these channels to divert the flow to any location within the bed. It is, however, also possible that the bypass is caused by the pulse of potassium branide (chemical formula) (KBr) when it is not properly mixed, and therefore, forms a pulse

Table 4. Hydraulic Parameters Calculated for the VSB

Port Number	Length (m)	*Pe*	$\overline{t_m}$ (h)	τ (h) [V/Q]	Time for 1st Peak (h)	Time for 2nd Peak (h)	Time for 3rd Peak (h)	Time for 4th Peak (h)	V_{eff}
1A & 1B	4	0.01	15.03	8.70	4.00	30.93			1.73
1	8	0.01	14.61	17.39	5.70	26.33			0.84
2A & 2B	12	2.47	20.35	26.09	8.93				0.78
2	16	5.10	22.21	34.78	15.00				0.64
3A & 3B	20	7.76	31.55	43.48	26.33				0.73
3	24	12.63	36.13	52.18	20.33	30.93			0.69
4A & 4B	28	17.67	41.47	60.87	35.93				0.68
4	32	8.26	37.89	69.57	15.00	30.93	42.72		0.54
5A & 5B	36	24.57	49.70	78.26	26.33	42.72			0.64
5	40	1.67	22.36	86.96	4.00	6.67	35.93	42.72	0.26

of liquid of a different density that typically travels along the base of the wetland. This effect has been described in various published articles on pond experiments,[30,34,35] where vertical stratification was found. This was ascribed to the variations in the salinity of an assortment of tracers at different flow rates. This effect is particularly noticeable in Port 5, which has a residence time which is much lower than that which we expect. This is shown in Table 4. We discuss this effect later.

Analysis of the Hydraulic Properties. An analysis of the modes of the distributions is presented in Figure 6. Theoretically, $\overline{t}_m$ must be directly proportional to length. The time taken for the peak of the RTD should also be directly proportional to the length of the VSR. This figure maps the progression of the peaks, that is, the time taken for the first peak and the ones that follow to pass. One can see that for the first peak there is a strong departure from linearity at the sample wells located at 24, 32, 36, and 40 m. However, if other modes are examined together with the first peak, the appearance of a linear relationship returns. Thus, if the first peak (or mode) is plotted from 0 to 20 m, the second peak for 24 m, the third peak for 32 m, the second peak for 36 m, and the fourth peak for 40 m, a linear relationship is observed (r^2=0.94) which is shown on the Figure. This means that the other modes of the age distribution for all sample ports can safely be assumed to represent bypass.

Within this figure, the Peclet number is also plotted with increasing distance. As the system behavior deviates strongly from ideal at 32 and 40 m (based on the bypass encountered in these sample ports) these have been excluded from the analysis. The *Pe* number can be fitted with a second-order polynomial with a high level of confidence (r^2=0.98, which, as the *Pe* number must display a squared relationship to length as discussed in literature, confirms that the Peclet equation is applicable to this system.[21]

The breakdown of the pulses of tracer into 1st, 2nd peak, and so forth, and the examination of the time taken for a given pulse to pass through the bed correlate quite closely to the measured residence time, $\overline{t}_m$. This implies that the fitted line presented above correlates to the primary pulse of tracer, and hence the flow.

The effective volume for each of the sampling ports is presented in Table 4. Given the almost constantly scaled ratio between the V/Q and $\overline{t}_m$, it is reasonable to assume that the nonideal behavior of the system is primarily attributable to dead volume. A smaller degree of short circuiting is evident during the initial stages (0–4 m) and at the tail of the reactor (36–40 m). This is shown by the deviation of linearity of $\overline{t}_m$ with respect to distance. The average effective volume calculated for this system was 75%. If the first 1 m and the final 4 m of the system are excluded, the average effective volume can be calculated at 69%. The implication is that between 25 and 31% of the designed volume of the reactor is not utilized.

To test our calculations, we used the methodology of Perrson et al.[31] to provide a comparison. Their equation was used to calculate hydraulic effectivity, as shown in Figure 7. For this VSR, the maximum hydraulic effectivity was calculated to be 0.64 or 64%. Hence, at most the system used 64% of its volume for effluent degradation purposes, while the remaining volume was essentially static or dead zones. This correlates reasonably well with our calculated effective volume of 69%.

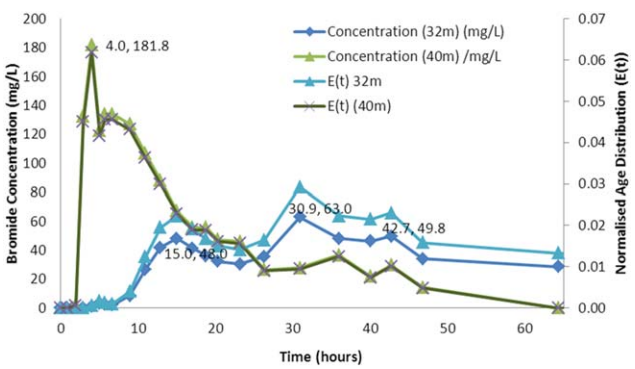

Figure 5. RTDs for sample ports at 32 and 40 m with multimodal distributions.

[Color figure can be viewed in the online issue, which is available at wileyonlinelibrary.com.]

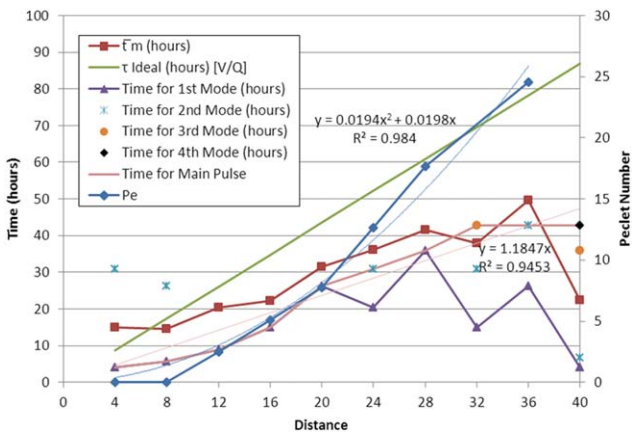

Figure 6. An analysis of the modes of distribution for the VSR.

[Color figure can be viewed in the online issue, which is available at wileyonlinelibrary.com.]

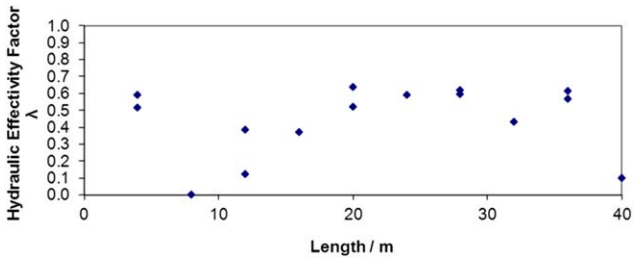

Figure 7. Hydraulic effectivity factor variation with length for each port within the VSR.

[Color figure can be viewed in the online issue, which is available at wileyonlinelibrary.com.]

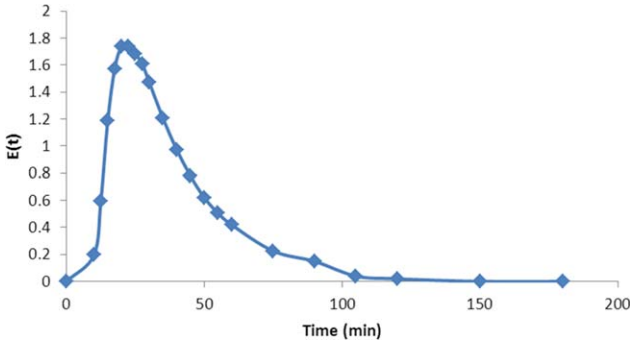

Figure 9. RTD for the impulse-response laboratory experiment.

[Color figure can be viewed in the online issue, which is available at wileyonlinelibrary.com.]

Hypothetical Reactor Volume. From the RTD curves, the initial stages of the VSR have a Gaussian-type distribution with a long tail, as discussed by Levenspiel[21] and also reported by others[12,36–39] for VSRs and packed-bed filters. This behavior indicates that the VSR can be represented using the Peclet model with dead zone(s) or as a series of tanks with dead volumes. We found that as the distance through the VSR increased, the bromide pulse became steadily degraded as other processes interfered with it. There were possible density effects from the impulse (which we attributed to poor mixing with the effluent as a result of differences in salinity and density, and/or bypass toward the end of the filter—sample port 5). We postulated that this was probably an effect of the density currents, which would be encountered only in the tracer experiment, and not in a well-mixed effluent stream arriving at the filter.

The experiment also showed that the behavior of the VSR deviates significantly from the ideal. This evidence includes the Figures showing the difference between $\bar{t}_m$ and τ, the relationship of the Peclet number with increments in length, the increase in residence time with length and the hydraulic effectivity as a function of length. For this system, the inactive volume of the VSR was found to be approximately 25%. We hypothesized that the dead zones can, especially in this case, be explained by investigating the location of the inlet and outlet port. In this filter, the outlet port is marginally lower than the inlet port. As the filter was full of liquid with no free surface runoff, the only way for the fresh influent to reach the bottom layers would be through deflection and diffusion. This would create preferential flow, with the greatest amount of flow occurring nearest the surface and in the center, and least flow occurring at the sidewalls and at the bottom. This is conceptualized as a hull-shaped velocity profile, which shown in Figure 8.

Calculation of the hydraulic properties of the laboratory-scale rig

Simulation of the Large-Scale CW—Flow Top to Top. The RTD for the laboratory reactor is shown in Figure 9. The RTD displays the typical behavior of a packed bed, as described above. This is the same type of behavior that was found for the VSR discussed earlier in this article, which implies that the systems are operating according to a fundamentally similar hydraulic regime.

A summary of the calculated hydraulic parameters for the laboratory reactor is presented in Table 5.

The laboratory reactor was calculated to have a Peclet number of approximately 4.8. This indicates that there are

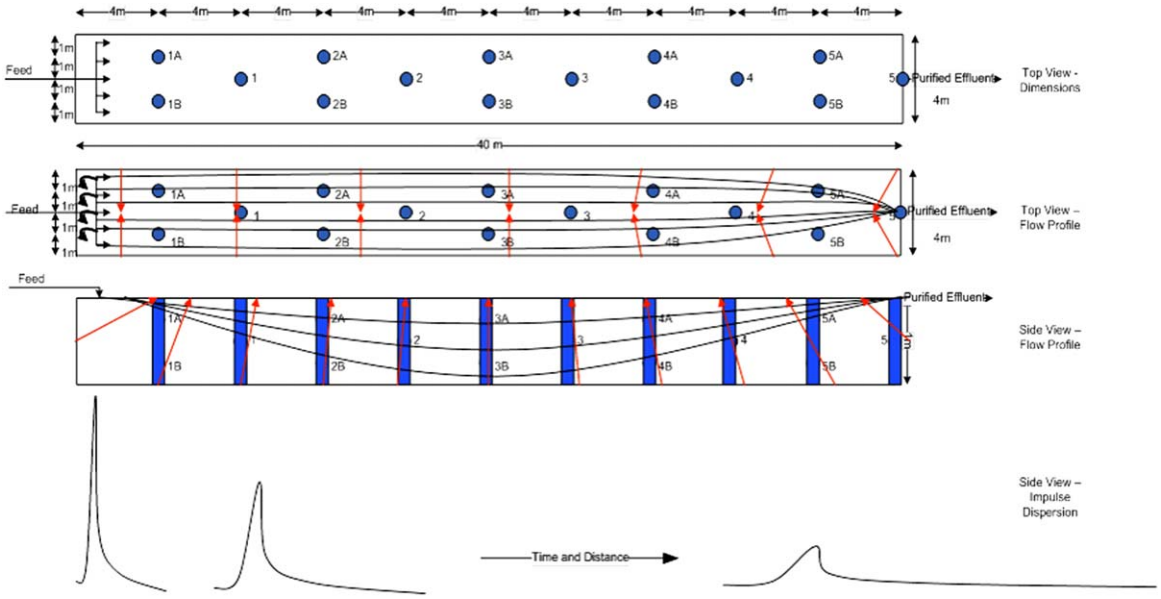

Figure 8. Hypothetical flow regime showing the boat-shaped velocity profile of tracer dispersion within the VSR.

[Color figure can be viewed in the online issue, which is available at wileyonlinelibrary.com.]

Table 5. Hydraulic Parameters for the Laboratory Apparatus

Parameter	Value
$\bar{t}_m$ (h)	0.616
τ (h) [V/F]	1.233
Time for 1st Peak (h)	0.375
V_{eff}	0.500
Pe	4.753

significant dispersive forces at work, and that the lab reactor is operating similarly to the VSR, although because of its shorter length, there is a significantly greater dead volume.

Having established mathematically that the laboratory apparatus is operating in a fundamentally similar manner to the VSR, we proposed that the hypothesis posited earlier for the VSR is valid for the laboratory apparatus. (In summation: there is a preferential flow, with the greatest flow occurring nearest the surface and in the center, and least flow occurring at the sidewalls and at the bottom; and that the flow can be conceptualized as a hull-shaped velocity profile.) Having used a transparent reactor and packing medium, we were able to photograph the tracer as it passed through the apparatus bed presented in Figure 10. Photograph A was taken during injection of the impulse of tracer; and Photograph B after 10 min as the tracer began to exit the apparatus. The distinctive hull-shaped profile of the dispersed tracer is clear, and has been accentuated in Photo B. Photograph C was taken after approximately an hour, and shows a new hull-shaped profile of clear liquid visibly replacing the dye.

Experiment to Test if the Hull-Shaped Profile could be Reduced by Distributing the Feed and the Outlet. The aim of this experiment was to test if it was possible to reduce dead volume by distributing the feed and outlet fully. In this experiment, the feed entered the rig via all nine inlet holes and exited through all nine outlet ports. The RTD for this experiment is shown in Figure 11.

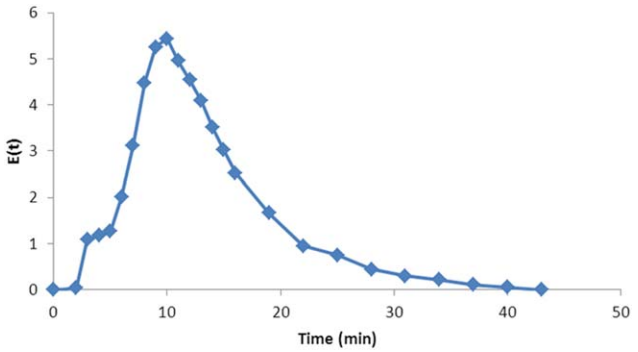

Figure 11. RTD for the impulse-response laboratory experiment with a well-distributed feed and outlet.

[Color figure can be viewed in the online issue, which is available at wileyonlinelibrary.com.]

A summary of the calculated hydraulic parameters for the laboratory reactor is presented in Table 6.

The laboratory reactor was calculated to have a Peclet number of approximately 6.7 for this experiment (i.e., $Pe = 6.7$). This value is significantly greater than that found in the experiment with feed and outlet located upon the surface. There was also a significant reduction in the dead volume in comparison to the experiment discussed earlier from 50 to 37.6%. This implies that the dead volume can be significantly reduced by distributing the feed and outlet lines. A

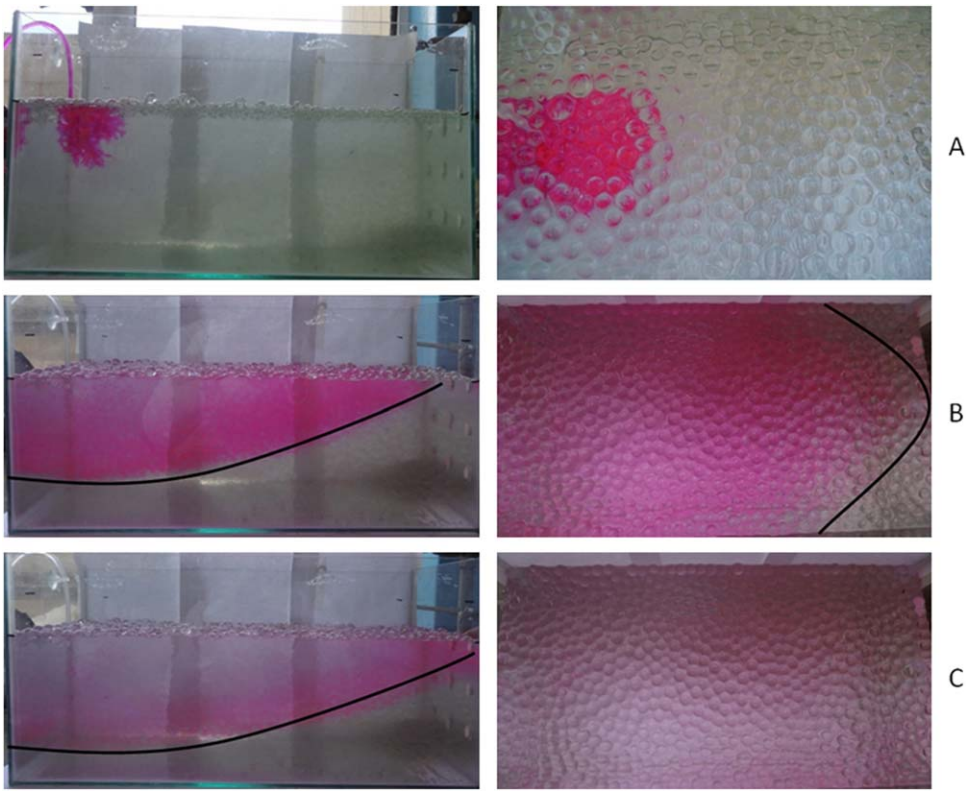

Figure 10. Photographs showing the flow patterns of tracer through the laboratory apparatus.

[Color figure can be viewed in the online issue, which is available at wileyonlinelibrary.com.]

Table 6. Hydraulic Parameters for the Laboratory Apparatus

Parameter	Value
$\overline{t_m}$ (h)	0.223
τ Ideal (h) [V/F]	0.308
Time for 1st Peak (h)	0.166
V_{eff}	0.724
Pe	6.667

photographic record of the experiment is presented in Figure 12. It is quite clear from this photo that the hull-shaped profile no longer exists.

Discussion of the results

Based on the data collected in this study, we believe that our hypothesis is indeed correct, that the flow in a VSR or any other packed-bed reactor has the following two properties; that it will carry on trying to go in the direction it started with some degree of dispersion that increases over distance; and that if the flow to such a system is upon the surface, and the outlet is also near the surface, the profile will be hull shaped. We note that the location of the inlet and outlet positions could also have a significant effect on the shape of this profile (as noted by other researchers[14]), or could even reduce the dead zone. It is believed that this hull-shaped velocity profile is a result of the fluid having low velocity and, thus, flow is laminar. If this is the case, there is no driver for the flow to mix or to move to the sides except for the deflective/dispersive forces from the packing medium. As the direction of these forces is random, the fluid will disperse; however, it cannot flow against gravity and must all flow out the outlet pipe. Hence, the fluid tapers toward the outlet creating the characteristic hull shape.

The focus of the research experiment described in this article was threefold: to report on the data we measured; to develop a hypothesis from the data obtained; and to test it. In summary the four components of the hypothesis included:

1. That there is a preferential flow pattern within a VSR, with the greatest flow occurring closest the surface and in the center, and the least at the sidewalls, if the flow is applied to the surface of the VSR at the feed position. This is conceptualized as a hull-shaped velocity profile. We believe this hypothesis is correct, and as far as we are aware flow pattern has not been described previously.
2. This profile is not dependent on the shape of the packing medium. The laboratory experiment confirms (at least with spherical packing materials) that the profile is not dependent on the packing if it is randomly distributed or if spherical packing materials are used in a VSR.
3. We can reproduce this hull-shaped profile in a laboratory-scale experiment using spherically shaped packing. We found that it was possible to induce the hull-shaped flow profile.
4. The profile can be changed by altering the location of the feed, and can be significantly reduced by introducing a fully distributed feed and outlet system. We found that it was possible to change the profile by modifying the feed and outlet distribution of the lab-scale rig, and that by doing so we could significantly reduce the dead volume and, thus, substantially increase the performance of the system.

Figure 12. Photographs showing the flow patterns of tracer through the laboratory apparatus.

[Color figure can be viewed in the online issue, which is available at wileyonlinelibrary.com.]

We conclude that hydraulic processes should be taken into account (i.e., not discounted or assumed to be ideal) in VSR calculations, and that the mean residence time is significantly different from the ideal residence time. This has significant consequences for any model which assumes that the hydraulic processes occurring within the system are ideal. The data that we measured indicate that for the optimal design of a bioreactor such as a VSR, the feed should be evenly distributed, and, even more important, the inlet and outlet from the VSR must be sufficiently well positioned to encourage flow through what in the experiments was identified as having the potential to be dead volume.

The design of a VSR that is efficient and relatively simple to maintain will fill the gap that exists at present between extremely sophisticated and expensive effluent treatment systems, and the more affordable low-technology wetland model. The water reclaimed can be used for irrigation, and the scale and effectiveness of the VSR design will be well suited to the needs of small-scale wineries.

What remains to be done in this research investigation (to estimate what effect the flow properties have on the effectiveness of the water treatment) will be the subject of a future article. The results of this stage of our work have indicated where the current design of the VSR can be improved from the hydraulic point of view, but we also require sufficient data to assess what chemicals remain in the treated water when the conventional VSR design is followed. Only once we combine these results can we come up with an optimal design for a VSR.

Notation

C = denotes concentration
C^* = background concentration
C_{Out} = exit concentration
C_{In} = inlet concentration
L_{In} = inlet organic load
L_{Out} = exit organic load
$L_{Removed}$ = load removed
X_i = conversion of component i
t_i = time i
t = the mean residence time for all components in PTIS model
θ = dimensionless time, $t/\bar{t}$
E_i = age at time i
D = dispersivity
τ = ideal mean residence time
$\bar{t}_m$ = mean of the RTD
λ = hydraulic efficiency factor
σ^2 = second moment of the RTD, the variance
σ^2_θ = dimensionless or normalized variance
N = number of tanks in a tanks-in-series model
P = apparent number of tanks in the apparent tanks-in-series model
k_i = rate constant for species i
b = time-based retardation coefficient
l = length of the bed
d = depth of the bed
w = width of the bed
V = volume of the CW
ε = void fraction of the gravel in the bed
V_{eff} = ratio derived from the ideal residence time to the real residence time
Pe = Peclet Number
Da = Damkohler Number

Literature Cited

1. Sheridan CM. A Critical Process Analysis of Wine Production to Improve Cost, Quality and Environmental Performance, M. Sc. Thesis. South Africa: University of Stellenbosch, 2003.
2. Government Gazette. Act No. 59 of 2008: National environmental management: Waste act, 2008. *Government Gazette*. 2009;525(32000).
3. Government Gazette. Act no. 36 of the National Water act of South Africa, Section 39, General Authorisations. *Government Gazette*. 2001.
4. Government Gazette. National Environmental Management Act. *Government Gazette*. 1998.
5. Government Gazette. National water Act, Act no 36 of 1998. *Government Gazette*. 1998.
6. Sheridan CM, Glasser D, Hildebrandt D. A calculation of the hydraulic properties of a vegetated gravel bed filter using an impulse-response tracer experiment to quantify non-ideal behaviour. In: Proceedings of the 12th International Conference on Environmental Science and Technology. Global Network on Environmental Science and Technology, Rhodes, Greece, 2011:1711–1716.
7. SAWIS. *South African Wine Industry Statistics (no.35)*. South African Wine Industry Statistics, South Africa. Accessed on May 25, 2012.
8. Malandra L, Wolfaardt G, Zietsman A, Viljoen-Bloom M. Microbiology of a biological contactor for winery wastewater treatment. *Water Res.* 2003;37:4125–4134.
9. Sheridan CM, Glasser D, Hildebrandt D, Petersen J, Rohwer J. An annual and seasonal characterisation of winery effluent in South Africa. *S Afr J Enol Vitic*. 2011;32(1):1–8.
10. Tchobanoglous G, Burton FL, Stensel HD, editors. Wastewater Engineering: Treatment and Reuse METCALF and Eddy, Inc. Revised, International Edition, 4th ed. New York: McGraw Hill, 2003.
11. Vohla C, Kõiv M, Bavor HJ, Chazarenc F, Mander Ü. Filter materials for phosphorus removal from wastewater in treatment wetlands—a review. *Ecol Eng*. 2011;37(1):70–89.
12. Werner TM, Kadlec RH. Wetland residence time distribution modeling. *Ecol Eng*. 2000;15(1–2):77–90.
13. Villaseñor J, Mena J, Fernández FJ, Gómez R, de Lucas A. Kinetics of domestic wastewater COD removal by subsurface flow constructed wetlands using different plant species in temperate period. *Int J Environ Anal Chem*. 2011;91(7–8):693–707.
14. Suliman F, Futsaether C, Oxaal U, Haugen LE, Jenssen P. Effect of the inlet–outlet positions on the hydraulic performance of horizontal subsurface-flow wetlands constructed with heterogeneous porous media. *J Contam Hydrol*. 2006;87(1–2):22–36.
15. Stein OR, Towler BW, Hook PB, Biederman JA. On fitting the k-C* first order model to batch loaded SSF wetlands. In: Proceedings of the 10th International Conference on Wetland Systems for Water Pollution Control. Lisbon, Portugal, 2006.
16. Sheridan CM, Peterson J, Rohwer J, Burton S. Engineering design of subsurface flow constructed wetlands for the primary treatment of winery effluent. In: Proceedings of the 10th International Conference on Wetland Systems for Water Pollution Control. Lisbon, Portugal, 2006.
17. Rousseau DPL, Vanrolleghem PA, De Pauw N. Model-based design of horizontal subsurface flow constructed treatment wetlands: a review. *Water Res*. 2004;38:1484–1493.
18. Martinez CJ, Wise WR. Analysis of constructed treatment wetland hydraulics with the transient storage model OTIS. *Ecol Eng*. 2003;20(3):211–222.
19. Kadlec RH. Effects of pollutant speciation in treatment wetlands design. *Ecol Eng*. 2003;20(1):1–16.
20. Carleton JN, Montas HJ. An analysis of performance models for free water surface wetlands. *Water Res*. 2010;44(12):3595–3606.
21. Levenspiel O. Chemical Reaction Engineering, International ed. Wiley, 1972.
22. Fogler HS. Elements of Chemical Reaction Engineering, 4th ed. USA: Prentice Hall, 2005.
23. Griffin DM Jr, Bhattarai RR, Xiang H. The effect of temperature on biochemical oxygen demand removal in a subsurface flow wetland. *Water Environ Res*. 1999;71(4):475–482.
24. Kadlec RH, Knight RL. Treatment Wetlands. Boca Raton, FL: CRC Press, 1996.
25. Reed SC, Brown D. Subsurface flow wetlands: a performance evaluation. *Water Environ Res*. 1995;67(2):244–248.
26. Vymazal J. Czech Constructed Wetlands Database. Ecology and Use of Wetlands. Prague, Czech Republic. 1998 [in Czech].
27. Wood A. Constructed wetlands in water pollution control: fundamentals to their understanding. *Water Sci Technol*. 1995;32(3):21–29.
28. Kadlec RH, Knight RL, Vymazal J, Brix H, Cooper P, Haberl R. *Constructed Wetlands for Pollution Control: Processes, Performance, Design and Operation*. Cornwall, UK: IWA Publishing, 2000.
29. Shepherd HL, Tchobanoglous G, Grismer ME. Time-dependent retardation model for chemical oxygen demand removal in a subsurface flow constructed wetland for winery wastewater treatment. *Water Environ Res*. 2001;73(5):597–606.

30. Chazarenc F, Merlin G, Gonthier Y. Hydrodynamics of horizontal subsurface flow constructed wetlands. *Ecol Eng*. 2003;21(2–3):165–173.
31. Perrson J, Somas NLG, Wong THF. Hydraulic efficiency of constructed wetlands and ponds. *Water Sci Technol*. 1999;40:291–299.
32. Popek EP. Sampling and Analysis of Environmental Chemical Pollutants—A Complete Guide. Academic Press, 2002.
33. Van Swaaij WPM, Charpentier JC, Villermaux J. Residence time distribution in the liquid phase of trickle flow in packed columns. *Chem Eng Sci*. 1969;24(7):1083–1095.
34. Schmid BH, Hengl MA, Stephan U. Salt tracer experiments in constructed wetland ponds with emergent vegetation: laboratory study on the formation of density layers and its influence on breakthrough curve analysis. *Water Res*. 2004;38:2095–2102.
35. Małoszewski P, Wachniew P, Czupryński P. Study of hydraulic parameters in heterogeneous gravel beds: constructed wetland in Nowa Słupia (Poland). *J Hydrol*. 2006;331(3–4):630–642.
36. Tanner CC, Sukias JPS, Upsdell MP. Organic matter accumulation during maturation of gravel-bed constructed wetlands treating farm dairy wastewaters. *Water Res*. 1998;32(10):3046–3054.
37. Kadlec RH. Comparison of free water and horizontal subsurface treatment wetlands. *Ecol Eng*. 2009;35:159–174.
38. Marsili-Libelli S, Checchi N. Identification of dynamic models for horizontal subsurface constructed wetlands. *Ecol Model*. 2005; 187(2–3):201–218.
39. Giraldi D, de'Michieli Vitturi M, Zaramella M, Marion A, Iannelli R. Hydrodynamics of vertical subsurface flow constructed wetlands: tracer tests with rhodamine WT and numerical modelling. *Ecol Eng*. 2009;35(2):265–273.

Manuscript received Mar. 19, 2013, and revision received Oct. 30, 2013.